Chiral Interactions in Polymer Liquid Crystals Reflecting Polymer Conformations: Triple-Helical Polysaccharide Schizophyllan and Poly(γ-benzyl L-glutamate)

Kazuto Yoshiba,* Akio Teramoto, and Naotake Nakamura

Department of Applied Chemistry, Faculty of Science and Engineering, Ritsumeikan University, Nojihigashi 1-1-1, Kusatsu, Siga 525-8577, Japan

Takahiro Sato

Department of Macromolecular Science, Osaka University, 1-1 Machikaneyama-cho, Toyonaka, Osaka 560-0043, Japan

Received September 30, 2002; Revised Manuscript Received December 30, 2002

ABSTRACT: Cholesteric pitch P was measured on D_2O solutions of a triple-helical polysaccharide schizophyllan as functions of temperature and concentration. The value of P varied with concentration and temperature and showed different concentration dependencies at lower and higher temperatures, with a sudden decrease in P in between. This is due to the order−disorder transition in schizophyllan solutions around 17 °C in D_2O. These data were analyzed by a statistical theory taking into account chiral repulsive and attractive interactions proposed by Sato et al. A subtle imbalance between the attractive and repulsive interactions gave rise to a large change in P. For the schizophyllan solutions, the attractive interaction changed according to the transition, while the change of the repulsive one was less remarkable. Similar analyses were performed on poly(γ-benzyl L-glutamate) data, elucidating the roles of the two interactions in determining the cholesteric structure.

1. Introduction

Robinson et al.[1,2] were the first to show that α-helical polypeptides form cholesteric lyotropic liquid crystals and characterized their structures in detail. Since then, there are many studies on lyotropic polymer cholesterics, including polypeptides and other rodlike or semiflexible polymers.[3−18] It is well-known that a nematic liquid crystal is transformed into a cholesteric one by chiral perturbations from other molecules in the vicinity.[19,20] This is also shown for achiral polyisocyanates doped with chiral polyisocyanates.[20,21]

The structure of a cholesteric liquid crystal is usually characterized by cholesteric pitch P or the cholesteric wavenumber q_c ($=2\pi/P$). Indeed, P has been measured for many polymer cholesterics, among which poly(γ-benzyl L-glutamate) (PBLG) has been studied extensively with respect to its dependence on temperature, polymer concentration, solvent, and so forth.[1−9] On the other hand, a cholesteric liquid crystal undergoes a structure change with different types of perturbation such as the conformational transition and so forth. A typical example is aqueous schizophyllan as reported previously.[22,23] The main chain of schizophyllan consists of three β-D-glucan chains wound into a triple helix, while each three units on the main chain have a side-chain glucose residue, which is connected to the main chain with a single bond and directed outward the helix core.[24−26] Because of this structure, schizophyllan mixes with water almost at all compositions, and aqueous schizophyllan undergoes an order−disorder transition at room temperature, with the ordered structure being formed with the side chain and water molecules in the vicinity.[22,23,27−35]

In this paper we report the change of cholesteric pitch P or q_c accompanying the transition in great detail. The concentration dependence of P is different at different temperatures, sandwiching the transition temperature in D_2O of 17 °C. Such data are analyzed by a theory of Sato et al.[36] on P, which takes into account the chiral repulsive and attractive interactions operating between polymer chains. The same analyses on data for PBLG solutions[4−8] are also attempted. The correlation between cholesteric structure and polymer conformation is discussed in terms of the results derived from such analyses.

2. Experimental Section

Two fractionated schizophyllan samples were prepared for cholesteric pitch measurements: sample KR-1A ($M_W = 23.7 \times 10^4$, $M_Z/M_W = 1.1_7$) and sample S21 ($M_V = 20.8 \times 10^4$). The weight-average molecular weights M_W and the z-average molecular weights M_Z for KR-1A in aqueous solution were determined at 25 °C on a Beckman Optima XL-I analytical ultracentrifuge equipped with a Rayleigh interference optical system ($\lambda_0 = 675$ nm) and charcoal-filled Epon 12 mm double-sector cells. The viscosity-average molecular weights M_V were determined from intrinsic viscosity at 25 °C using the $[\eta]-M_W$ relationship established by Yanaki et al.[25]

The cholesteric pitch of schizophyllan in D_2O was determined by 488 and 633 nm light diffraction and polarized microscopy with a thermostatic cell holder.[14,15,23] A polymer solution for the cholesteric pitch measurements was filled in a drum-shaped glass cell with a thin inlet tube. The temperature was monitored by a thermocouple attached on the cell wall. When compared, the P values from three methods agreed within ±2%. The refractive index for D_2O solution necessary for the analysis of the diffraction data was calculated from $dn/dc = 0.151$ cm^3 g^{-1} measured on an Optilab DSP along with the refractive index at higher concentrations determined by an Abbe refractometer. When the temperature was jumped from 20 to 10 °C, P was found to change very gradually on all D_2O solutions, and the equilibrium P value was attained only after 2000 min from the temperature jump. Once the equilibrium value was achieved, it did not change even if the solution was cooled from 15 to 10 °C or heated from 5 to 10 °C. For

10.1021/ma021538n CCC: $25.00
Published on Web 02/27/2003

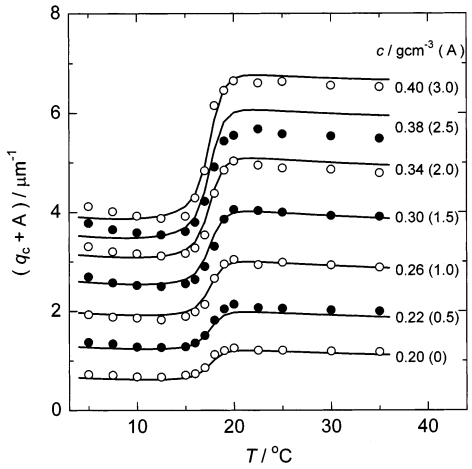

Figure 1. Temperature dependence of cholesteric pitch P for D_2O solutions of KR-1A at concentrations of 0.20−0.40 g/cm^3. Solid curves represent theoretical values calculated by eq 1 with the chiral interaction parameters $\lambda\Delta$ and δ^* estimated from smooth curves connecting the data points obtained by the curve-fitting method in Figure 4. The data points and curves are shifted vertically by the values in the parentheses for viewing clarity.

this reason, equilibrium values in the transition region (16−19 °C) were determined only on the heating process.

3. Results

In Figure 1, the equilibrium cholesteric wavenumber q_c (=$2\pi/P$) is plotted against temperature for KR-1A−D_2O solutions of different concentrations. It is seen that q_c shows a steady decrease with temperature at lower and higher temperatures and undergoes a sharp transition around 17 °C at each concentration. As shown in the previous papers,[22,23] this transition is accompanied by the order−disorder transition of schizophyllan solutions detected by optical rotation, heat capacity, and so forth.[22,23,27−35]

We found that the transition also changes the polymer concentration dependence of P. As shown in Figure 2A, P for KR-1A−D_2O solutions decreases monotonically with the polymer mass concentration c above 18 °C but seems to take a minimum at $c \sim 0.35$ g/cm^3 below 15 °C. This unusual concentration dependence of P is however not unique to schizophyllan solutions but was observed by Toriumi et al.[4−8] in *m*-cresol and 1,2,3-trichloropropane solutions of PBLG at high temperatures (cf. Figure 5), which exhibited no thermal conformational transition.

Figure 2B compares the concentration dependence of P for D_2O and H_2O solutions of schizophyllan at 10 and 30 °C. Here, the H_2O solution is known to exhibit the order−disorder transition at ca. 7 °C, so that the schizophyllan triple helix is in the disorder state in H_2O at both 10 and 30 °C. Because of this isotope effect, the data points of H_2O solutions at 10 °C (as well as at 30 °C) obey the curve for D_2O solutions at 30 °C, and the concentration dependence of P is very different in D_2O and H_2O solutions of schizophyllan at 10 °C. This indicates that the twisting interactions between cholesteric layers are changed by the order−disorder transition.

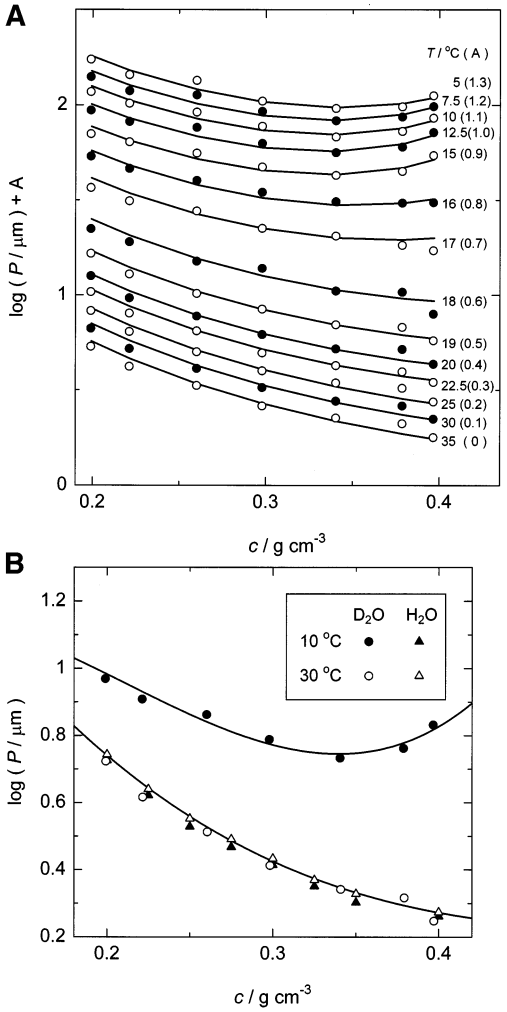

Figure 2. (A) Polymer concentration dependence of cholesteric pitch P for D_2O solutions of KR-1A at temperatures of 5−35 °C. Solid curves represent the least-squares fitting by eq 1 (see text) with the molecular parameters of schizophyllan: M_L = 2150 nm^{-1}, d = 1.75 nm, q = 200 nm.[35] The data points and curves are shifted vertically by the values in the parentheses. (B) Comparison of cholestric pitch for KR-1A−D_2O and S21−H_2O solutions at 10 and 30 °C. Solid curves are the same as those in panel A at the same temperatures.

Discussion

A. Schizophyllan Solutions. The cholesteric pitch P is determined by the balance of the chiral twisting force and elastic force against the twist deformation. Sato et al.[36,37] formulated the Frank elastic force constants and P for lyotropic polymer liquid crystals, taking the polymer flexibility effect into account using the equivalent freely jointed chain model (EFJC). Here, the EFJC is defined as a freely jointed chain of which orientational order parameter in a liquid crystalline solution is identical with that of the wormlike cylinder with the same contour length in the same solution. The theoretical results were favorably compared with experimental P and the elastic constants of various lyotropic polymer liquid crystals, including P data of aqueous schizophyllan in the disorder state. In this section, we analyze P data of schizophyllan solutions in the entire temperature range encompassing the order−disorder transition using this theory.

The twisting force between polymer chains may arise from chiral both repulsive and dispersion (or attractive) interactions, as pointed out by Straley,[37] Samulski and Samulski,[39] and Osipov.[40−42] The former and latter interactions may be characterized by the depth Δ of helical groove and the strength δ^* of the chiral disper-

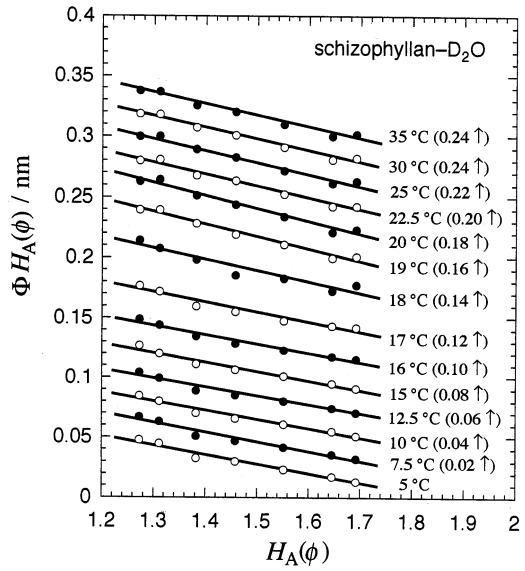

Figure 3. Plots of $\Phi H_A(\phi)$ vs $H_A(\phi)$ for KR-1A−D_2O solutions at different temperatures, constructed from the data shown in Figure 2A. Solid lines represent the least-squares fitting. The data points and curves are shifted vertically by the values in the parentheses.

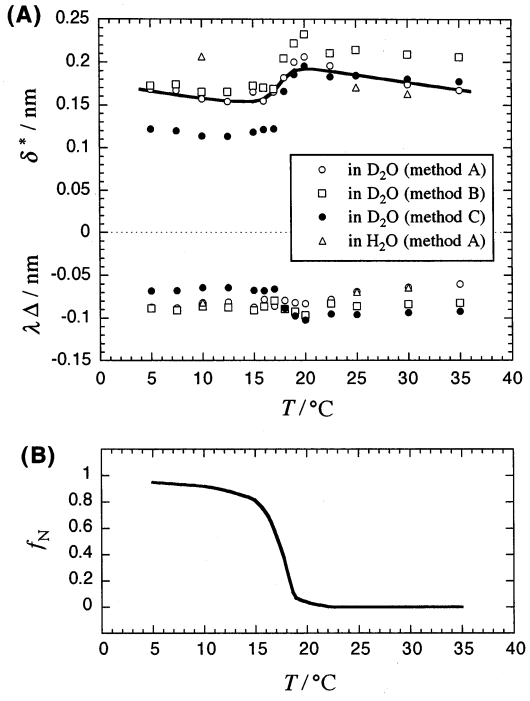

Figure 4. (A) Temperature dependencies of $\lambda\Delta$ and δ^* derived by analyzing concentration dependence of cholesteric pitch for D_2O and H_2O solutions of the schizophyllan sample KR-1A; unfilled circles, squares, and filled circles are the results obtained for the D_2O solution by the curve-fitting method (method A), the $\Phi-H_A(\phi)^{-1}$ plot (method B), and the $\Phi H_A(\phi)-H_A(\phi)$ plot (method C), respectively; triangles are the results obtained for the H_2O solution by the curve-fitting method, and the solid curve is drawn using eq 3. (B) Fraction f_N of monomer units in the ordered state of the schizophyllan triple helix in D_2O, calculated according to ref 35.

sion force of the polymer chain, respectively. Those chiral interactions operative between the rodlike segments of the EFJC are incorporated into the free energy of the system, and the free energy is minimized with respect to the twisting angle, yielding the equilibrium P or the cholesteric wavenumber q_c as[36]

$$2\pi/P = q_c = [6S^2/\kappa^2 I_2(S)][\lambda\Delta + \delta^*/H_A(\phi)] \quad (1)$$

Here, S is the orientational order parameter in the cholesteric solution, κ is the segment length of the EFJC, ϕ is the polymer volume fraction in the solution, λ is a numerical constant of order of unity, and $I_2(S)$ and $H_A(\phi)$ are known functions of S and ϕ, respectively.[36,37] Values of S and κ can be calculated as functions of ϕ using the wormlike cylinder parameters, the molar mass per contour length M_L, the persistence length q, and the diameter d.

According to eq 1, with the known values for the wormlike cylinder parameters of the schizophyllan triple helix (M_L = 2150 nm^{-1}, q = 200 nm, and d = 1.75 nm),[24−26] the concentration dependence of P is calculated given the two chiral interaction parameters $\lambda\Delta$ and δ^*. In the previous study, this equation was used to analyze the $P-c$ relation by a linear plot of $\Phi \equiv q_c[\kappa^2 I_2(S)/6S^2]$ vs $1/H_A(\phi)$. On the other hand, it is rearranged to give another linear relation of $\Phi H_A(\phi)$ vs $H_A(\phi)$ by multiplying $H_A(\phi)$ on both sides of eq 1. In principle, both these equations allow to estimate the two parameters separately. Of course, the parameters may be also estimated by a simple curve fitting which minimizes σ defined by

$$\sigma^2 = n^{-1}\sum_{i=1}^{n}\left(\ln \frac{|P^{\text{experiment}}(c_i)|}{|P^{\text{theory}}(c_i)|}\right)^2 \quad (2)$$

for P data at various concentrations c_i at a fixed temperature, where n is the number of experimental data points (i.e., $1 \le i \le n$) and the superscripts experiment and theory refer to theoretical and experimental P values, respectively. Here, we have assumed that errors in experimental P are proportional to the magnitude of P. This method may properly access experimental errors in P, but the contributions of the chiral repulsive and attractive interactions to P cannot be seen explicitly in the plot.

The solid curves in Figure 2A represent the theoretical values for P obtained by the least-squares fitting method for KR-1A−D_2O solutions. It is seen that the theoretical curve follows closely the data points at each temperature. On the other hand, Figure 3 shows the linear plot of $\Phi H_A(\phi)$ vs $H_A(\phi)$ for the same data. All the lines indicated were drawn by the least-squares method. Although not shown, we obtained similar linear plots of Φ vs $1/H_A(\phi)$ from the same pitch data. Similar analyses were performed also on data for H_2O solutions of schizophyllan.

The chiral interaction parameters $\lambda\Delta$ and δ^* for D_2O solutions of schizophyllan determined by the three methods are plotted against temperature in Figure 4A. Although the three different methods provide appreciably different values of $\lambda\Delta$ and δ^*, we can definitely see a general trend that the change of δ^* at low and high temperatures is linear with temperature but is abrupt in the vicinity of the order−disorder transition temperature (∼17 °C). On the other hand, as shown by triangles in Figure 4, δ^* of schizophyllan in H_2O shows only a gradual temperature dependence above 10 °C, outside the transition region. Thus, the change of δ^* in the transition region can be linearly related to the fraction f_N of monomer units of schizophyllan in the ordered state. Theoretically, f_N is a function of N, T, the transition enthalpy ΔH_r, the transition temperature T_r^∞,

Table 1. Chiral Interaction Parameters of Helical Polymers

polymer[a]	solvent[b]	$\lambda\Delta$/nm	δ^*/nm	method[c]	ref
schizophyllan	D_2O (10 °C)^{ord}	−0.083	0.156	A	present study
schizophyllan	H_2O (10 °C)^{dis}	−0.082	0.21	A	present study
schizophyllan	D_2O (25 °C)^{dis}	−0.067	0.184	A	present study
schizophyllan	H_2O (25 °C)^{dis}	−0.063	0.17	B	36
PBLG	*m*-cresol (20 °C)	−0.0070	0.020	B	present study
PBLG	*m*-cresol (120 °C)	0.035	−0.063	B	present study
PBLG	TCP (40 °C)	0.028	−0.031	B	present study
PBLG	TCP (100 °C)	0.0385	−0.059	B	present study
PBLG	dioxane (22, 25 °C)	−0.0051	0.017	B	36
PNIC	toluene (43.7 °C)	−0.028	0.0735	B	36

[a] PNIC = poly{(*R*)-2,6-dimethylheptyl isocyanate}; TCP = 1,2,3-trichloropropane. [b] dis = disordered; ord = ordered. [c] Methods: A, curve fitting; B, linear plot of Φ vs $H_A(\phi)^{-1}$.

and cooperativity parameter σ. Using the ΔH_r, T_r^∞, and σ of D_2O solutions of schizophyllan given in ref 35, f_N for KR-1A ($N = 122$) has been calculated (see Figure 4B). The solid curve in Figure 4A represent the δ^*-T relation constructed by combining those in the three regions:

$$\delta^*/\mathrm{nm} = -0.061 f_N + 160.5/(T/\mathrm{K}) - 0.353 \quad (3)$$

Contrarily, the change of $\lambda\Delta$ is less remarkable, and we can see no clear temperature dependence of $\lambda\Delta$ determined by the curve-fitting method (method A) and the Φ vs $1/H_A(\phi)$ plot (method B); only the results obtained from the plot of $\Phi H_A(\phi)$ vs $H_A(\phi)$ (method C) exhibit a small jump around 17 °C similar to δ^*. The latter plot gives the value of $\lambda\Delta$ as the slope, which may be estimated more consistently from the data of different temperatures than the other methods. From these results, we conclude that the order−disorder transition in aqueous schizophyllan changes the chiral interactions among the helices as expected. This is confirmed also in Table 1.

B. PBLG Solutions. Toriumi et al.[6−8] extensively studied the temperature and concentration dependencies of the cholesteric pitch for *m*-cresol and 1,2,3-trichloropropane (TCP) solutions of poly(γ-benzyl L-glutamate) (PBLG). Their results are shown in Figure 5, where the concentration dependence of P changes systematically with temperature similar to those shown in Figure 2, but the system becomes nematic (i.e., $q_c = 0$ or $P = \infty$) at some temperatures in both solvents. The curve-fitting and linear plot methods have been used for the analysis. Figure 6 shows the linear plot of Φ vs $1/H_A(\phi)$ for *m*-cresol solutions of PBLG at different temperatures, as an example. The data points almost follow a straight line at each temperature, from which we have determined the chiral interaction parameters of PBLG α-helix as functions of temperature. The solid curves in Figure 5 are drawn using the parameters determined by the linear plot. It is seen that the theory describes the complicated behavior of P rather precisely; the present analysis needs a certain number of data points, and the data at some temperatures have been omitted because they do not fulfill this condition.

Temperature dependencies of $\lambda\Delta$ and δ^* of the PBLG α-helix obtained in *m*-cresol and TCP by the linear plot are shown in Figure 7; the curve-fitting method gave essentially the same temperature dependencies. Although slightly scattered, the data points of both $\lambda\Delta$ and δ^* look to follow smooth lines in both solvents with no symptom of transition. The temperature dependencies of $\lambda\Delta$ and δ^* of PBLG are as weak as those of schizophyllan except in the transition region, as shown in Figure 1 below 15 °C or above 20 °C. These gradual temperature dependencies may be ascribed to gradual changes in the side-chain conformation and/or the degree of solvation with temperature.

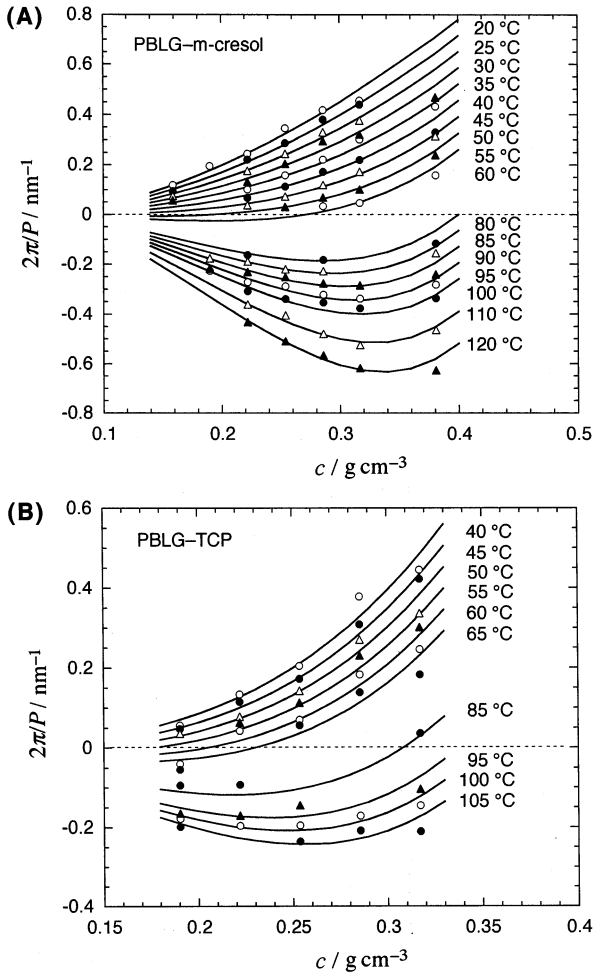

Figure 5. Concentration dependencies of cholesteric pitch of the systems (A) PBLG−*m*-cresol (the viscosity average molecular weight = 2.46×10^5) and (B) PBLG−TCP (the viscosity average molecular weights = 1.84×10^5 and 2.46×10^5). Symbols, experimental data;[6−8] solid curves, theoretical values calculated by eq 1 with the chiral interaction parameters determined by the linear plot (cf. Figure 7) and the molecular parameters of PBLG: $M_L = 1450$ nm^{-1}, $d = 1.42$ nm, $q = 150$ nm.[36]

The signs of $\lambda\Delta$ and δ^* of both schizophyllan and PBLG are opposite each other, except in a very narrow temperature region (around 30 °C) for *m*-cresol solutions of PBLG. This means that the chiral repulsive and attractive interactions twist cholesteric layers in the opposite direction. This relation of the two twisting

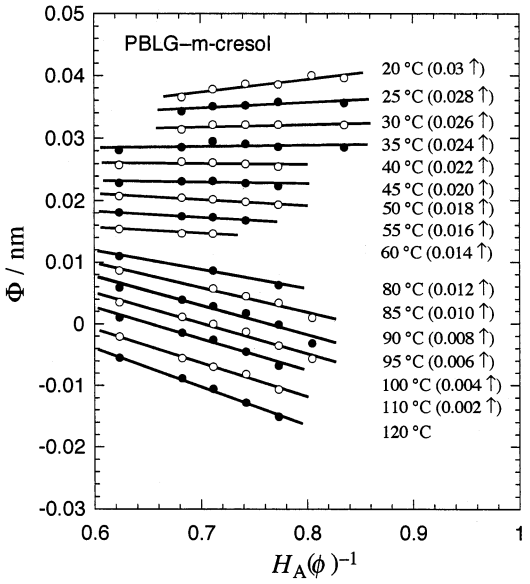

Figure 6. Plots of Φ vs $H_A(\phi)^{-1}$ for PBLG−*m*-cresol solutions at different temperatures, constructed from the data shown in Figure 5A. Solid lines represent the least-squares fitting. The data points and curves are shifted vertically by the values in the parentheses.

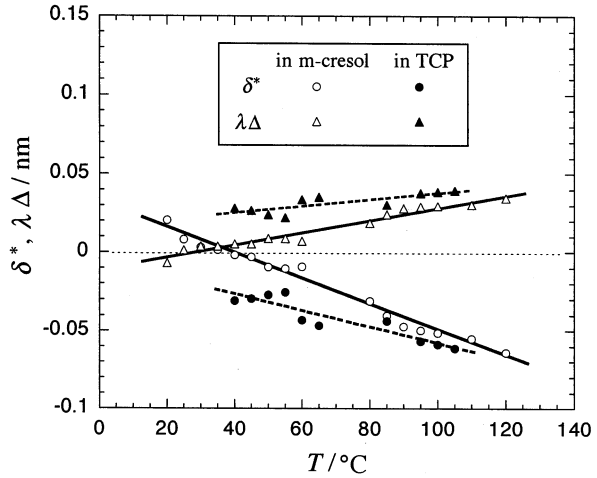

Figure 7. Temperature dependencies of $\lambda\Delta$ and δ^* for the systems PBLG−*m*-cresol (unfilled symbols) and PBLG−TCP (filled symbols) determined from the linear plot of Φ vs $H_A(\phi)^{-1}$.

forces holds also for other lyotropic polymer liquid crystal systems (cf. Table 1), but we cannot theoretically verify it at present. As seen from eq 1, the cholesteric pitch is determined by the compensation of the chiral repulsive and attractive twisting forces. For schizophyllan and PBLG solutions analyzed, the attractive twisting force surpasses the repulsive one in most cases. The opposite case is found only in the PBLG−TCP solution below 60 °C and the PBLG−*m*-cresol solution at 40−60 °C.

Since absolute values of the repulsive and attractive terms in eq 1 are not so much different for all the systems listed in Table 1, a subtle imbalance between the two terms with the opposite sign causes a large change cholesteric structure. In other words, a minute change in the microscopic level gives rise to a large change in macroscopic structure. As a result, the cholesteric pitch of schizophyllan solutions in Figure 1 changes more remarkably in the transition region than $\lambda\Delta$ and δ^* in Figure 4.

It is noted that the signs of $\lambda\Delta$ and δ^* of PBLG in *m*-cresol change at ca. 35 °C, indicating that the twisting forces arising both from chiral repulsive and attractive interactions change the direction at that temperature. However, this does not mean the thermal inversion of the PBLG α-helix sense. The sign of $\lambda\Delta$ is determined not only by the helical groove sense but also by the pitch and width of the groove and also helix diameter as pointed out by Gottarelli et al.[43] According to Osipov,[40−42] δ^* depends on the frequency-dependent anisotropies of the molecular polarizability and of the gyration tensor, which may change the signs by local side-chain conformation especially by the orientation of the phenyl ring of PBLG.

Abe and Yamazaki[44] studied the side-chain conformation of PBLG in *m*-cresol as well as in 1,4-dioxane and chloroform over 30−80 °C by deuterium NMR combined with the rotational isomeric-state analysis. They obtained an asymmetric population of the gauche$^+$ and gauche$^-$ conformations at the low temperature for outer bonds of the side chain and also a very much different stable side-chain conformation in *m*-cresol from those in the other solvents. These results imply that the unique side-chain conformation of PBLG in *m*-cresol may be responsible for the thermally driven inversion of the twisting force direction in the cholesteric phase. However, differing from aqueous schizophyllan, the NMR data show no cooperative transition. This is consistent with the monotonic changes in $\lambda\Delta$ and δ^* for these systems. Finally, it must be stressed that although $\lambda\Delta$ and δ^* are the main competing factors, the competition is greatly amplified by the concentration factors in eq 1, yielding a remarkable change in *P*.

Acknowledgment. This work was in part supported by the CREST of Japan Science and Technology A.T. thanks Yamashita Sekkei Co. Ltd. for the chair-professorship at Ritsumeikan University.

References and Notes

(1) Robinson, C.; Ward, J. C.; Beevers, R. B. *Discuss. Faraday Soc.* **1958**, *25*, 29.
(2) Robinson, C. *Tetrahedron* **1961**, *13*, 219.
(3) DuPre, D. B.; Duke, R. W. *J. Chem. Phys.* **1975**, *63*, 143.
(4) Uematsu, Y.; Uematsu, I. In *Mesomorphic Order in Polymers*; ACS Symposium Series No. 74; American Chemical Society: Washington, DC, 1978; Chapter 1.
(5) Uematsu, I. *Koubunshi* **1978**, *27*, 754−757.
(6) Toriumi, H.; Yahagi, K.; Uematsu, I. *J. Polym. Sci., Polym. Phys. Ed.* **1980**, *19*, 1167−1169.
(7) Toriumi, H.; Minakuchi, S.; Uematsu, I. *Mol. Cryst. Liq. Cryst.* **1983**, *94*, 267−284.
(8) Uematsu, I.; Uematsu, Y. *Adv. Polym. Sci.* **1985**, *41*, 35.
(9) Itou, S. *Mol. Cryst. Liq. Cryst.* **1989**, *172*, 201.
(10) Senechal, E.; Maret, G.; Dransfeld, K. *Int. J. Biol. Macromol.* **1980**, *2*, 256.
(11) Tseng, S.-L.; Valente, A.; Gray, G. D. *Macromolecules* **1981**, *14*, 715.
(12) Laivins, G. V.; Gray, G. D. *Macromolecules* **1985**, *18*, 1746.
(13) Guo, J.-X.; Gray, G. D. *Macromolecules* **1989**, *22*, 2082.
(14) Van, K.; Norisuye, T.; Teramoto, A. *Mol. Cryst. Liq. Cryst.* **1981**, *78*, 123.
(15) Itou, T.; Van, K.; Teramoto, A. *J. Appl. Polym. Sci., Appl. Polym. Symp.* **1984**, *16*, 165.
(16) Yanaki, T.; Norisuye, T. Teramoto, A. *Polym. J.* **1984**, *16*, 165−173.
(17) Sato, T.; Teramoto, A. In *Ordering in Macromolecular Systems*; Teramoto, A., Kobayashi, M., Norisuye, T., Eds.; Springer-Verlag: Berlin, 1994; pp 155−169.
(18) Sato, T.; Teramoto, A. *Adv. Polym. Sci.* **1996**, *126*, 85−161.
(19) Sato, T.; Sato, Y.; Umemura, Y.; Teramoto, A.; Nagamura, Y.; Wagner, Y.; Weng, D.; Okamoto, Y.; Hatada, K.; Green, M. M. *Macromolecules* **1993**, *26*, 4551−4559.

(20) Green, M. M.; Zanella, S.; Gu, H.; Sato, T.; Gottarelli, G.; Spada, G. P.; Schoevaars, A. M.; Ferigna, B.; Teramoto, A. *J. Am. Chem. Soc.* **1998**, *120*, 9810−9817.
(21) Gu, H. Ph.D. Thesis, Osaka University, 1997.
(22) Asakawa, T.; Van, K.; Teramoto, A. *Mol. Cryst. Liq. Cryst.* **1984**, *166*, 129−139.
(23) Teramoto, A.; Yoshiba, K.; Nakamura, N.; Nakamura, J.; Sato, T. *Mol. Cryst. Liq. Cryst.* **2001**, *365*, 373−380.
(24) Norisuye, T.; Yanaki, T.; Fujita, H. *J. Polym. Sci., Polym. Phys. Ed.* **1980**, *18*, 547−558.
(25) Yanaki, T.; Norisuye, T.; Fujita, H. *Macromolecules* **1980**, *13*, 1462−1466.
(26) Norisuye, T. *Makromol. Chem. Suppl.* **1985**, *14*, 105−118.
(27) Itou, T.; Teramoto, A.; Matsuo, T.; Suga, H. *Macromolecules* **1986**, *19*, 1234−1240.
(28) Itou, T.; Teramoto, A.; Matsuo, T.; Suga, H. *Carbohydr. Res.* **1987**, *160*, 243−257.
(29) Kitamura, S.; Kuge, T. *Biopolymers* **1989**, *28*, 639−654.
(30) Kitamura, S.; Ozawa, M.; Tokita, H.; Hara, C.; Ukai, S.; Kuge, T. *Thermochim. Acta* **1990**, *163*, 89−96.
(31) Hirao, T.; Teramoto, A.; Matsuo, T.; Suga, H. *Biopolymers* **1990**, *29*, 1867−1876.
(32) Teramoto, A.; Gu, H.; Miyazaki, Y.; Sorai, M. *Biopolymers* **1995**, *36*, 803−810.
(33) Miura, N.; Yagihara, S.; Mashimo, S.; Gu, H.; Teramoto, A. *Proc. Jpn. Acad.* **1998**, *74*, 1−5.
(34) Hayashi, Y.; Shinyashiki, N.; Yagihara, S.; Yoshiba, K.; Teramoto, A.; Nakamura, N.; Miyazaki, Y.; Sorai, M. *Biopolymers* **2002**, *63*, 21−31.
(35) Yoshiba, K.; Ishino, T.; Teramoto, A.; Nakamura, N.; Miyazaki, Y.; Sorai, M.; Hayashi, Y.; Shinyashiki, N.; Yagihara, S. *Biopolymers* **2002**, *63*, 370−381.
(36) Sato, T.; Nakamura, J.; Teramoto, A.; Green, M. M. *Macromolecules* **1998**, *31*, 1398−1405.
(37) Sato, T.; Teramoto, A. *Macromolecules* **1996**, *29*, 4107−4114.
(38) Straley, J. P. *Phys. Rev. A* **1976**, *14*, 1835.
(39) Samulski, T. V.; Samulski, E. T. *J. Chem. Phys.* **1977**, *67*, 824.
(40) Osipov, M. A. *Chem. Phys.* **1985**, *96*, 259.
(41) Osipov, M. A. *Il. Nuovo Cimento D* **1988**, *10*, 1249.
(42) Osipov, M. A. In *Liquid Crystalline and Mesomorphic Polymers*; Shibaev, V. P., Lam, L., Eds.; Springer: Berlin, 1994; Chapter 1.
(43) Gottarelli, G.; Spada, G. P.; Garbesi, A. In *Comprehensive Supramolecular Chemistry*; Lehn, J.-M., Ed.; Pergamon: Oxford, 1996; Vol. 9, p 483.
(44) Abe, A.; Yamazaki, T. *Macromolecules* **1989**, *22*, 2138, 2145.

MA021538N